Journal of Biomolecular NMR, **19:** 355–360, 2001.
KLUWER/ESCOM

3D H_{aro}-NOESY-CH_3NH and C_{aro}-NOESY-CH_3NH experiments for double labeled proteins

Youlin Xia, David Man & Guang Zhu*
Department of Biochemistry, The Hong Kong University of Science and Technology, Clear Water Bay, Kowloon, Hong Kong

Received 16 November 2000; Accepted 8 February 2001

Key words: aromatic protons, CH_2-filtering, HSQC, NOESY

Abstract

Precision in the determination of the 3D structures of proteins by NMR depends on obtaining an adequate number of NOE restraints. Ambiguity in the assignment of NOE cross peaks between aromatic and other protons is an impediment to high quality structure determination. Two pulse sequences, 3D H_{aro}-NOESY-CH_3NH and 3D C_{aro}-NOESY-CH_3NH, based on a modification of a technique for simultaneous detection of ^{13}C-^1H (of CH_3) and ^{15}N-^1H correlations in one measurement, are proposed in the present work. These 3D experiments, which are optimized for resolution in the ^{13}C and ^{15}N dimensions, provide NOE information between aromatic protons and methyl or amide protons. CH_2 moieties are filtered out and the CH groups in aromatic rings are selected, allowing their NOE cross peaks to be unambiguously assigned. Unambiguous NOEs connecting aromatic and methyl or amide protons will provide important restraints for protein structure calculations.

Multidimensional and multinuclear NMR spectroscopy can successfully determine the 3D structures of double or triple labeled proteins with molecular weights up to 30 kDa (Bax, 1994; Kay and Gardner, 1997). Nevertheless, the structure determination of many proteins of biological importance remains challenging with current NMR techniques (Zwahlen et al., 1998). The main difficulty is still the assignment of NOE cross peaks to specific and proximal proton pairs.

In order to overcome the problem of ambiguous distance restraints arising from overlapping NOE cross peaks, an elegant computational method called ARIA (Ambiguous Restraints for Iterative Assignment) (Nilges, 1995; Nilges et al., 1997) has been developed. An alternative and complementary approach, using a novel isotope labeling strategy, i.e. ^{15}N, ^{13}C, and ^2H-labeling with methyl protonation (Metzler et al., 1996; Zwahlen et al., 1998a, b) or $^1H_\alpha$-protonation (Yamazaki et al., 1997), has also been developed. The latter strategy is still very costly, although a robust and cost-effective method for the production of methyl-protonated triple labeled proteins has been proposed (Goto et al., 1999).

Because methyl-containing amino acids are abundant in proteins, the assignment of inter-residue NOEs arising from methyl-containing side chains plays an important role in determining the NMR structures of proteins. NOESY experiments, which allow definitive assignments of NOEs between methyl and other protons to be made, are valuable for uniformly ^{13}C and ^{15}N labeled protein samples. Recently, a 3D NOESY experiment (Uhrin et al., 2000) using CH_2 filtering has been proposed to detect NOEs between methyl or amide protons and other protons. Since aromatic ring-containing amino acids also occur frequently in proteins, and the proton resonance peaks of aromatic spin systems often overlap with those of amide protons, the ability to partition aromatic proton resonances and amide proton resonances into separate dimensions in 3D spectra will be especially helpful for the reliable assignment of these NOE cross peaks.

In this work, two pulse sequences, a 3D H_{aro}-NOESY-CH_3NH and a 3D C_{aro}-NOESY-CH_3NH,

*To whom correspondence should be addressed. E-mail: gzhu@ust.hk

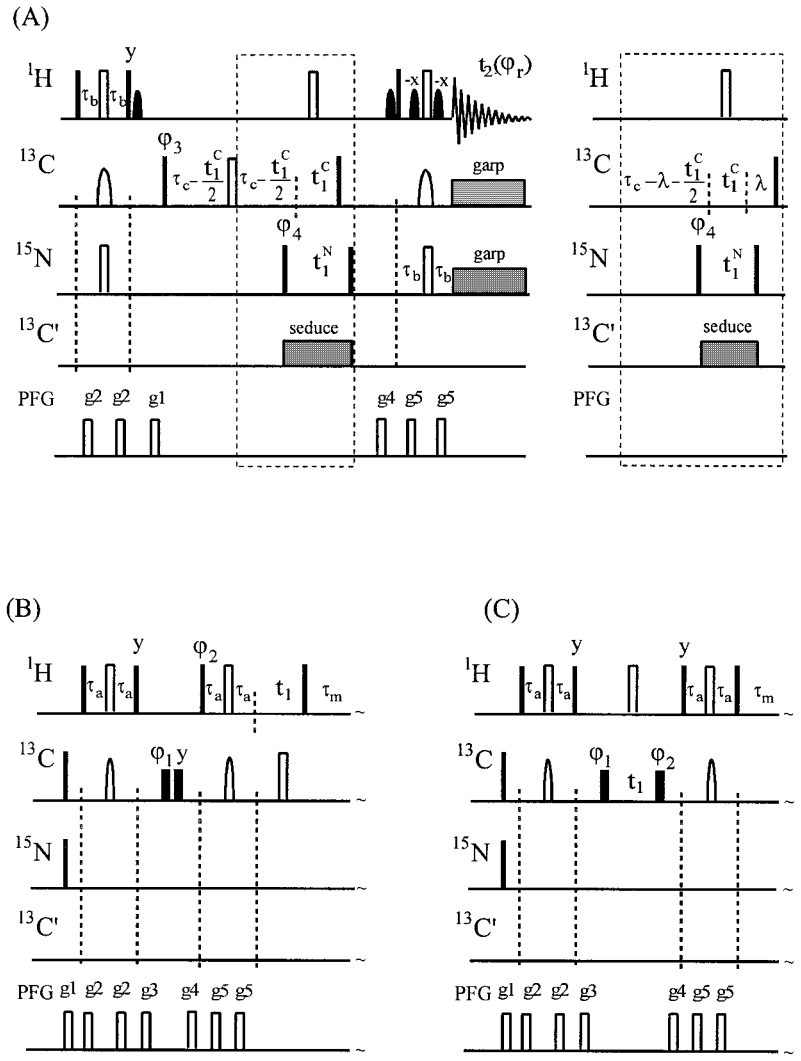

Figure 1. Pulse sequences of the 2D HSQC-CH_3NH (A), 3D H_{aro}-NOESY-CH_3NH (B) and C_{aro}-NOESY-CH_3NH (C). The section in the dashed box of the sequence in (A) is replaced with that at the right of (A) for every third and fourth scan. The sequences in (B) and (C) are continued by the sequence in (A) with the exception that t_1 and t_2 are changed to t_2 and t_3, respectively. For all sequences, filled bars and open bars represent 90° and 180° pulses, respectively. Filled shaped pulses are 1.1 ms sinc-modulated rectangular 90° pulses to selectively excite the water resonance. The ^{1}H and ^{13}C carrier frequencies were centered at 7.1 and 127 ppm for aromatic rings before the NOE mixing period, and 4.7 and 19.6 ppm for methyl groups after the NOE mixing period. The ^{15}N carrier frequency was centered at 120 ppm. The widths of the two 90° ^{13}C pulses with lower rf power in (B) and (C) are 66 μs. The ^{13}C shaped pulses for aromatic carbons and methyl carbons are 0.48 ms and 0.96 ms iburp2 180° pulses (Geen and Freeman, 1991). Phase-modulated SEDUCE ^{13}C′ decoupling was adopted during the t_1 period in (A). $\tau_a = 1/(4^1J_{CH(aro)}) = 1.43$ ms, $\tau_b = 2.27$ ms, $\tau_c = 1/(2^1J_{CC}) = 14.3$ ms, $\lambda = 1/(2^1J_{CH3}) = 4.0$ ms, $\tau_m = 150$ ms. Recovery delays between scans were set to 1.0 s. The default phases are x. For (A), the phase cycling was: $\varphi_3 = (x,-x)$; $\varphi_4 = (x,-x,-x,x)$; $\varphi_r = (x,-x,-x,x)$. Quadrature components in t_1^C and t_1^N were acquired through setting $\varphi_3 = \varphi_3 - 90°$ and $\varphi_4 = \varphi_4 + 90°$, respectively. Axial peaks in the F_1^C and F_1^N dimensions were removed by inverting (φ_3, φ_r) and (φ_4, φ_r) for every second t_1^C and t_1^N increment, respectively. For (B) and (C), the phase cycling was: $\varphi_1 = 4(y),4(-y)$; $\varphi_2 = 8(y),8(-y)$; $\varphi_3 = (x,-x)$; φ_4=(x,−x,−x,x); $\varphi_r = (x,-x,-x,x,-x,x,x,-x,-x,x,x,-x,x,-x,-x,x)$. The quadrature components in t_1, t_2^C and t_2^N were acquired through setting $\varphi_2 = \varphi_2 - 90°$, $\varphi_3 = \varphi_3 - 90°$ and $\varphi_4 = \varphi_4 + 90°$, respectively. For (B) and (C), the axial peaks in the F_1, F_2^C and F_2^N dimensions were removed by inverting (φ_2, φ_r) or (φ_1, φ_r), (φ_3, φ_r) and (φ_4, φ_r) for every second t_1, t_2^C and t_2^N increment, respectively. The durations and strengths of the gradients are g1=(0.4 ms, 15 G/cm); g2=(0.4 ms, 5 G/cm); g3=(0.4 ms, 10 G/cm); g4=(0.4 ms, 15 G/cm), and g5=(0.3 ms, 8 G/cm).

based on a modification of a technique for simultaneous detection of ^{13}C-^{1}H (of CH_3) and ^{15}N-^{1}H correlations in one measurement (Uhrin et al., 2000), are proposed. These two experiments can provide NOE information between aromatic protons and methyl or amide protons. Both types of NOEs can be obtained in a single experimental measurement. One advantage of these experiments is that there are no diagonal peaks, simplifying the assignment of NOE resonances, and the resolution of ^{13}C and ^{15}N can be simultaneously optimized.

Figure 1 depicts the pulse sequences of (A) the 2D HSQC-CH_3NH, (B) the 3D H_{aro}-NOESY-CH_3NH and (C) the 3D C_{aro}-NOESY-CH_3NH experiment. For every third and fourth scan, the section in the dashed box in the 2D HSQC-CH_3NH sequence (Figure 1A) is replaced with the sub-sequence in the dashed box at the right of Figure 1A. In the 3D H_{aro}-NOESY-CH_3NH and 3D C_{aro}-NOESY-CH_3NH experiments, the pulse sequence shown in Figure 1A is appended to those in Figures 1B and 1C, respectively, with the exception that t_1 and t_2 in Figure 1A are changed to t_2 and t_3, respectively.

The 2D HSQC-CH_3NH pulse sequence (Figure 1A) has been modified from an earlier proposed method (Uhrin et al., 2000). In the sequence described here, different spectral widths for the ^{13}C of the methyl groups and ^{15}N can be set to optimize the spectral resolution of ^{13}C and ^{15}N in the 2D HSQC-CH_3NH experiment and the two 3D experiments. To enhance spectral resolution in the ^{13}C dimension and for CH_2 filtering, constant time evolution in the t_1 period is used, as shown in the sequence in Figure 1A.

As the CH_3 group of methionine residues does not have a one-bond ^{13}C-^{13}C scalar coupling and $\tau_c = 1/(2^1J_{CC}) = 14.3$ ms ($^1J_{CC} = 35$ Hz), $\cos(2\pi^1 J_{CC}\tau_c) = -1$, the cross peak related to the CH_3 of methionine residues is negative, if the peaks of other residues containing CH_3 groups are positive. Therefore, the CH_3 of methionine residues can easily be distinguished from other methyl-containing residues in the 2D HSQC-CH_3NH, 3D H_{aro}-NOESY-CH_3NH and 3D C_{aro}-NOESY-CH_3NH spectra.

CH_2 filtering (Uhrin et al., 2000) has been used in the proposed pulse sequences to remove spectral overlaps between CH_3 and CH_2 groups. This was achieved by using one-bond ^{13}C-^{1}H scalar coupling and an appropriate phase cycling scheme, as specified in the caption of Figure 1. For the first two scans of the sequence shown in Figure 1A, carbons were decoupled from protons, and the transverse magnetization of ^{13}C was not modulated by the one-bond ^{13}C-^{1}H scalar coupling. In other words, the modulation factors of the transverse magnetizations of ^{13}C for the CH, CH_2 and CH_3 groups due to the one-bond ^{13}C-^{1}H scalar coupling were 1, 1 and 1, respectively. For the next two scans (in which the sub-sequence in the dashed box at the right of Figure 1A replaces the section in the dashed box in the sequence in Figure 1A), the effective one-bond ^{13}C-^{1}H scalar coupling time was 2λ, and the modulation factor for the transverse magnetization of ^{13}C was $\cos^n(2\pi^1 J_{CHn}\lambda)$ for each CH_n. As $\lambda = 1/(2^1J_{CH3}) = 4.0$ ms, the modulation factors were almost -1, $+1$, and -1 for the CH, CH_2, and CH_3 groups, respectively.

Thus, with four-step phase cycling with φ_3 = (x, $-$x), φ_4 = (x,$-$x,$-$x,x), φ_r = (x,$-$x,$-$x,x), two steps of which result in isotope filtering (Cavanagh et al., 1995), the magnetization of the CH_2 group is cancelled, while those of the CH and CH_3 groups are retained. In employing this CH_2-filtering method, the signal strength of CH_3 is not reduced compared with the method used before (Uhrin et al., 2000). In addition, the signal of CH_α is also filtered out, because the carrier frequency of ^{13}C in the 2D HSQC-CH_3NH (Figure 1A) is centered at 19.6 ppm, which is far from the $^{13}C_\alpha$ resonance frequency, and the inversion profile ($\geq$96%) of the two 960 μs iburp2 (Geen and Freeman, 1991) shaped pulses only extends from 8.6 to 30.6 ppm. In order to avoid exciting CH_3 groups in the sequences depicted in Figures 1B and 1C before the NOE mixing period, the widths of the two 90° pulses were set to 66 μs. Two 480 μs iburp2 shaped pulses were applied to further reduce the excitation of CH_3. The inversion profile ($\geq$96%) of these iburp2 pulses extends from 149–105 ppm.

In Figure 1B, a refocused INEPT sequence has been applied to filter out the magnetization of the amide and aliphatic protons but to retain the magnetization of the aromatic protons. Signals from the aromatic protons were frequency-labeled in the t_1 period, and then their longitudinal magnetization was mixed with that of the methyl or amide protons during the NOE mixing period. The magnetization of the methyl or amide protons was then transferred to their attached methyl carbons or amide nitrogens through the first INEPT in the 2D HSQC-CH_3NH sequence. They were frequency-labeled with methyl carbon and amide nitrogen frequencies in the t_2 (t_1 in Figure 1A) period. The second INEPT of the 2D HSQC-CH_3NH section transferred the anti-phase magnetization of the methyl carbons and amide nitrogens to their attached

methyl or amide protons. Finally, their transverse magnetizations were frequency-labeled and detected during the t_3 (t_2 in Figure 1A) period.

In Figure 1C, only the aromatic carbons were frequency-labeled in the t_1 period. The longitudinal magnetization of the aromatic carbon-attached protons was then mixed with that of other protons during the NOE mixing period. For the ∼17 kDa test sample used here (calmodulin) there was no TROSY (Pervushin et al., 1998, 2000; Meissner and Sørensen, 1999) effect with the aromatic spin systems, so the ^{13}C evolution mode of the HSQC sequence was utilized, as shown in Figure 1C. For larger proteins, TROSY-based sequences can be applied to the ^{15}N-^{1}H groups, and the ^{13}C-^{1}H groups in aromatic spin systems.

To effectively demonstrate the two proposed 3D NOESY experiments for detecting NOEs between aromatic protons and methyl or amide protons, we applied them to a uniformly ^{15}N and ^{13}C labeled calmodulin sample (∼17 kDa, 1.5 mM in 6.1 mM $CaCl_2$ and 0.1 M KCl, pH 6.3, 95% H_2O/5% D_2O) of high concentration using a Varian Inova 750 MHz NMR spectrometer at 47 °C. All data processing was performed using the NMRPipe software package (Delaglio et al., 1995).

The 2D HSQC-CH_3NH experiment combined constant time in ^{13}C (methyl carbon) and variable time in ^{15}N (amide nitrogen) for frequency labeling. Therefore the correlation between the $^{13}C_{CH3}$ and $^{1}H_{CH3}$ of the methyl groups and between ^{15}N and $^{1}H_N$ of the amide groups could be simultaneously detected, and optimized in resolution, in one experiment. Signals were maximized when τ_b was set to 2.17 ms and 2.38 ms for the CH_3 and the NH moieties, respectively. However, τ_b was set to 2.27 ms in normal experiments as a compromise. Using this value, the signals were 99.6% and 98.8% of their maxima for the CH_3 and the NH moieties, respectively. The spectral widths of the indirect detection dimensions in the 2D HSQC-CH_3NH experiment were set to 3150 Hz and 2400 Hz, which correspond to the full spectral widths of the methyl ^{13}C and ^{15}N on a 750 MHz spectrometer, respectively.

Two 3D H_{aro}-NOESY-CH_3NH and C_{aro}-NOESY-CH_3NH spectra were acquired. Data matrices in the time domain were composed of $32^*\times32^*\times512^*$ points and $32^*\times32^*\times512^*$ points (* signifies complex points), with spectral widths of $1800\times3150\times$ 10500 Hz and $3770\times3150\times$ 10500 Hz for the 3D H_{aro}-NOESY-CH_3NH and the 3D C_{aro}-NOESY-CH_3NH experiments, respectively. The spectral widths of ^{15}N were set to 2400 Hz in the two 3D experiments. The numbers of scans for each transient were 64 and 48 for the H_{aro} and C_{aro} experiments, respectively. Cosine bell window functions were applied to the two 3D spectra before Fourier transformation. The processed spectra were composed of $128\times128\times1024$ points. If the resolution in the ^{13}C dimension is not an issue, the constant-time (t_2) period can be replaced by a normal evolution period in order to increase sensitivity of these experiments. Since the proposed experiments are longer than the 3D and 4D $^{13}C/^{13}C$ or $^{13}C/^{15}N$ separated NOESY experiment, the sensitivities of these experiments are generally lower.

The 2D [$^{1}H_{aro}$-$^{1}H_N$] (F_1-F_3) slice and the 2D [$^{1}H_{aro}$-$^{1}H_{CH3}$] (F_1-F_3) slice of the 3D H_{aro}-NOESY-CH_3NH spectrum taken at ^{15}N chemical shift $F_2 = 118.68$ ppm and $^{13}C_{CH3}$ chemical shift $F_2 = 23.34$ ppm are shown in Figures 2A and 2B. The 2D [$^{13}C_{aro}$-$^{1}H_N$] (F_1-F_3) slice and the 2D [$^{13}C_{aro}$-$^{1}H_{CH3}$] (F_1-F_3) slice of the 3D C_{aro}-NOESY-CH_3NH spectrum taken at ^{15}N chemical shift $F_2 = 118.68$ ppm and $^{13}C_{CH3}$ chemical shift $F_2 = 23.34$ ppm are shown in Figures 2C and 2D, respectively. Because only the aromatic signals are indirectly detected in the t_1 dimension for these 3D spectra, the number of cross peaks is limited. Therefore these NOE cross peaks could easily and unambiguously be assigned. For the test sample, there were one histidine, two tyrosine, eight phenylalanine and zero tryptophan residues. The spectral dispersion in the $^{1}H_{aro}$ dimension of the 3D H_{aro}-NOESY-CH_3NH spectrum was better than that in the $^{13}C_{aro}$ dimension of the 3D C_{aro}-NOESY-CH_3NH spectrum, as shown in Figures 2A and 2C. The chemical shifts of $^{13}C_{aro}$ for the phenylalanine residues were near 132.5 ppm. These two 3D experiments are complementary and there should be a one to one correspondence between the NOE cross peaks in the two 3D spectra, thereby providing definitive NOE connections.

In conclusion, two pulse sequences, the 3D H_{aro}-NOESY-CH_3NH and the 3D C_{aro}-NOESY-CH_3NH, based on a modification of a technique for simultaneously detecting ^{13}C-^{1}H (in CH_3), and ^{15}N-^{1}H correlations in one measurement, are proposed. The different spectral widths of ^{13}C in CH_3 and ^{15}N can be set to optimize the spectral resolution in the 2D HSQC-CH_3NH section of the two proposed 3D experiments. Since the chemical shifts of C_β of Val and Ile, C_γ of Leu are closer to those of methyl carbons and far away from the C_α chemical shifts, NOE cross peaks connecting these carbon-attached

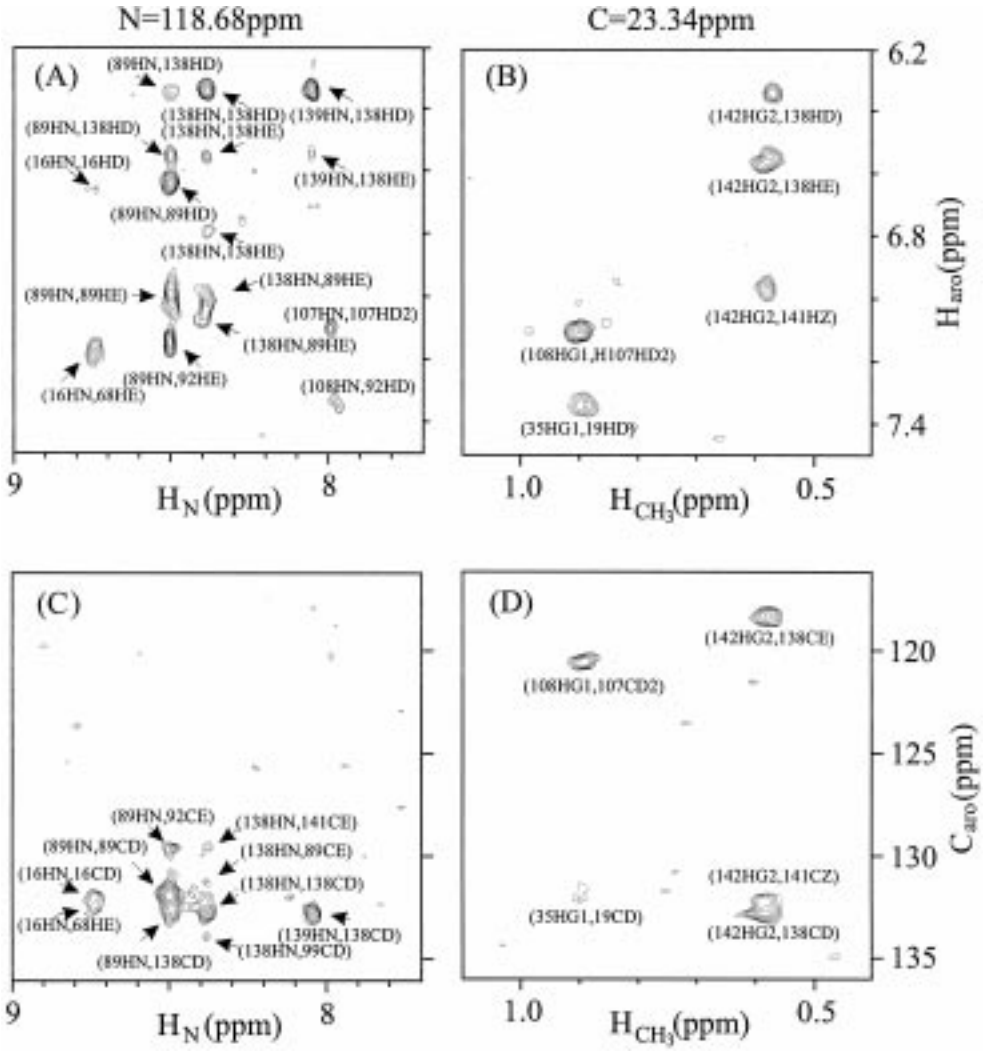

Figure 2. 2D [$^1H_{aro}$-^1H_N] (F_1-F_3) slice (A) and 2D [$^1H_{aro}$-$^1H_{CH3}$] (F_1-F_3) slice (B) of the 3D H_{aro}-NOESY-CH_3NH spectrum taken at ^{15}N chemical shift F_2 = 118.68 ppm and $^{13}C_{CH3}$ chemical shift F_2 = 23.34 ppm, respectively. 2D [$^{13}C_{aro}$-^1H_N] (F_1-F_3) slice (C) and 2D [$^{13}C_{aro}$-$^1H_{CH3}$] (F_1-F_3) slice (D) of the 3D C_{aro}-NOESY-CH_3NH spectrum taken at ^{15}N chemical shift F_2 = 118.68 ppm and $^{13}C_{CH3}$ chemical shift F_2 = 23.34 ppm, respectively. The lowest contours for spectra (A) and (B) are drawn at the same level, and for (C) and (D) the lowest contours are also identical. Contours are separated by a factor of 1.24.

protons and aromatic protons are present in our proposed 3D experiments. The intensities of these NOE peaks are 33% of those NOE peaks connecting methyl protons and aromatic protons, which are insignificant in most cases. Although the number of unambiguous NOE restraints that can be obtained is dependent on the resolution and assignments of the aromatic resonances, two proposed 3D experiments can give NOE information between aromatic protons and methyl or amide protons, and provide a powerful means to obtain definite NOE restraints for the determination of 3D structures of proteins.

Acknowledgements

This work was supported in part by grants to G.Z. from the Research Grants Council of Hong Kong (HKUST6038/98M, 6199/99M and 6208/00M). The Hong Kong Biotechnology Research Institute is acknowledged for the purchase of the 750 MHz NMR spectrometer. The authors thank Dr. K.H. Sze and Dr. David Smith for their kind help and valuable discussions.

References

Bax, A. (1994) *Curr. Opin. Struct. Biol.*, **4**, 738–744.

Cavanagh, J., Fairbrother, W.J., Palmer III, A.G. and Skelton, N.J. (1995) *Protein NMR Spectroscopy, Principles and Practice*, Academic Press, San Diego, CA.

Delaglio, F., Grzesiek, S., Vuister, G., Zhu, G., Pfeifer, J. and Bax, A. (1995) *J. Biomol. NMR*, **6**, 277–293.

Geen, H. and Freeman, R. (1991) *J. Magn. Reson.*, **93**, 93–141.

Goto, N.K., Gardner, K.H., Mueller, G.A., Willis, R.C. and Kay, L.E. (1999) *J. Biomol. NMR*, **13**, 369–374.

Kay, L.E. and Gardner, K.H. (1997) *Curr. Opin. Struct. Biol.*, **7**, 722–731.

Meissner, A. and Sørensen, O.W. (1999) *J. Magn. Reson.*, **139**, 447–450.

Metzler, W.J., Wittekind, M., Goldfarb, V., Mueller, L. and Farmer, B.T. (1996) *J. Am. Chem. Soc.*, **118**, 6800–6801.

Nilges, M. (1995) *J. Mol. Biol.*, **245**, 645–660.

Nilges, M., Macias, M.J., O'Donoghue, S.I. and Oschkinat, H. (1997) *J. Mol. Biol.*, **269**, 408–422.

Pervushin, K., Riek, R., Wider, G. and Wüthrich, K. (1998) *J. Am. Chem. Soc.*, **120**, 6394–6400.

Pervushin, K., Braun, D., Fernández, C. and Wüthrich, K. (2000) *J. Biomol. NMR*, **17**, 195–202.

Uhrin, D., Bramham, J., Winder, S.J. and Barlow, P.N. (2000) *J. Biomol. NMR*, **18**, 253–259.

Yamazaki, T., Tochio, H., Furui, J., Aimoto, S. and Kyogoku, Y. (1997) *J. Am. Chem. Soc.*, **119**, 872–880.

Zwahlen, C., Gardner, K.H., Sarma, S.P., Horita, D.A., Byrd, R.A. and Kay, L.E. (1998a) *J. Am. Chem. Soc.*, **120**, 7617–7625.

Zwahlen, C., Vincent, S.J.F., Gardner, K.H. and Kay, L.E. (1998b) *J. Am. Chem. Soc.*, **120**, 7617–7625.